On the Intensity of Atmospheric Convection

J. Oerlemans

Institute for Meteorology and Oceanography, University of Utrecht, Princetonplein 5, UTRECHT, The Netherlands

(Manuscript received 15.12.1982, in revised form 11.03.1983)

Abstract:

Several runs with a numerical cloud model are discussed in order to quantify the effect of latent heat release on the development of convective activity averaged over some region. A scheme of the numerical results is constructed by means of a simple gradient system, with surface heat flux and moisture content as control parameters. For some range of these control parameters, two stable steady states occur. Internal forcing due to latent heat release creates the bifurcation.

On the basis of Monte Carlo integrations with the gradient system it is shown that for moist conditions convective activity tends to have a bimodal probability distribution. The practical consequence is that the short-range predictability of the weather is substantially reduced.

Zusammenfassung: Über die Intensität atmosphärischer Konvektion

Die Arbeit diskutiert mehrere Rechenläufe mit einem numerischen Wolkenmodell, um den Effekt der Freisetzung latenter Wärme auf die Entwicklung der konvektiven Aktivität quantitativ zu untersuchen. In einem Schema der numerischen Ergebnisse, konstruiert mit Hilfe eines einfachen Gradientsystems, dienen der Wärmefluß und der Feuchtegehalt an der Oberfläche als Steuerparameter. In einem bestimmten Bereich dieser Parameter gibt es zwei stabile stationäre Zustände. Die Bifurkation wird intern durch das Freisetzen latenter Wärme erzwungen.

Mit Hilfe von Monte-Carlo-Integrationen mit dem Gradientsystem wird gezeigt, daß für feuchte Bedingungen die konvektive Aktivität zu einer bimodalen Wahrscheinlichkeits-Verteilung tendiert. Die praktische Konsequenz ist eine beträchtliche Verminderung der kurzfristigen Vorhersagbarkeit des Wetters.

Résumé: Sur l'intensité de la convection atmosphérique.

On présente plusieurs essais avec un modèle numérique de nuage, en vue de quantifier l'effet de la libération de chaleur latente sur le développement de l'activité convective, en moyenne sur une région. Dans un schéma des résultats numériques, construit à l'aide d'un simple système à gradient, on utilise le flux de chaleur et l'humidité en surface comme paramètres de contrôle. Dans un domaine déterminé de ces paramètres, il y a deux états stationnaires stables. La contrainte interne due à la libération de chaleur latente crée la bifurcation.

Sur la base d'intégrations par la méthode de Monte – Carlo, on montre que dans l'air humide, l'activité convective tend à avoir une distribution en probabilité bimodale. La conséquence pratique en est que la prédictabilité du temps à court terme est substantiellement réduite.

1 Introduction

In many atmospheric situations the (thermo) dynamics of the troposphere are dominated by *convection.* On the average the radiation balance of the atmosphere is negative, and that of the earth surface is positive. The balancing upward flux of latent and sensible heat is accomplished by convection. Averaged over the globe and over the year, this upward heat flux amounts to about 30 % of the incoming solar energy at the top of the atmosphere (e. g. GATES, 1981). Although the action of convection is thus very important

0005-8173/83/03 0341-13 $ 02.00/0

in the global energy budget, it has a moderate scale: much smaller than the scale of motion in which one is interested when studying the general circulation of the atmosphere (or designing a large-scale numerical forecast model). In view of this it is not surprising that atmospheric convection may be dealt with in many different ways.

In modelling the large-scale circulation in the atmosphere one is particularly interested in how convection modifies the vertical temperature structure of the atmosphere, but limited computer capacity makes it impossible to carry out an explicit calculation. This has led to the development of so-called convective parameterization schemes (e. g. ARAKAWA and SCHUBERT, 1974; KUO, 1974). Another topic involving bulk properties of atmospheric convection is the growth of the convective boundary layer during daytime, which is of importance with regard to air pollution problems. When the air is so dry that no condensation takes place, the evolution of such a convective boundary layer can be well described by simple models (e. g. DRIEDONKS, 1982).

The heart of the matter, of course, is the dynamics of moist atmospheric convection. A good deal of research has been carried out in this field, in particular since it became feasible to integrate the dynamic equations in time with the aid of high-speed computers. Examples of studies on the structure of atmospheric convection are: BROWNING and LUDLAM (1962), TELFORD and WARNER (1962), KITCHEN and CAUGHEY (1981) [observational studies]; MURRAY (1970), MILLER (1978), MONCRIEFF (1978, 1981) [model studies]; to name but a few.

From a global point of view, three modes can be distinguished in atmospheric convection. First we have the case that no condensation takes place. The degree of predictability is high: both the depth of the convective layer and the mean kinetic energy in this layer depend on the (time-dependent) boundary conditions in a smooth way.

Things become much more complicated when the lower atmosphere contains a substantial amount of water vapour. Upward motions may now lead to the formation of cumulus clouds and latent heat is released. This internal heat generation, which depends on the motion field itself, will strongly affect the dynamics of the convection. So the same heat flux may now initiate much stronger motions. In addition to this, large cumulus clouds generate strong downdraughts (by evaporative cooling at the cloud edges and by momentum exchange with falling precipitation in showers), and these downdraughts act as additional internal forcing. In short, the presence of sufficient water vapour leads to positive feedback once a specific level of convective activity has been reached. This can be considered as the second mode of atmospheric convection.

The third, and generally most energy containing mode, results from organization of convective clouds. This organization can either represent a free or a forced mode. An example of a free mode is the formation of cellular cloud patterns in convection in a cold air mass flowing over a warm ocean. Increased convection on a sea-breeze front, or in tropical easterly waves, can be seen as examples of forced organization.

It may very well be that in a sufficiently moist atmosphere multiple statistically steady circulation states occur. Statistically steady here means that the level of kinetic energy, averaged over a sufficiently large area, is essentially constant. When conditions are suitable, latent heat release and downdraughts being internally generated can easily keep convection going, even when the surface heat flux is zero or negative (but provided that moisture is always available). For a negative surface heat flux, however, an atmosphere at rest will remain so. As will be illustrated by results from a numerical cloud model, the structure of atmospheric convection is such that multiple steady states indeed occur.

The purpose of this paper is to demonstrate that the presence of moisture leads to bifurcation of statistical equilibria of a convective atmospheric layer, and to investigate the consequences with regard to predictability of convective activity. To this end an attempt will be made to describe the behaviour of the model convective layer in terms of a simple gradient system of the type

$$\dot{V} = f(V, F, \Delta), \tag{1}$$

where V is the rms air velocity, the dot denotes derivative with respect to time, F is the sensible heat flux at the surface and Δ is in some way a measure of the moisture content of the atmospheric layer involved. So the kinetic energy of the motion (V is just the square root of it) is supposed to be the best quantity to characterize the state of the convective layer. With Equation (1), only a modelling of the time and space averaged state is attempted. The time interval and domain size over which an average is taken should at least be several times the typical time scale and space scale of a thermal, or of a cumulus cloud when condensation occurs.

It is of course difficult to describe accurately the rich and complex behaviour of moist convection in this simple way. For instance, it is very well possible that a very long time integration with a numerical model of moist convection would reveal the existence of periodic solutions. Equation (1) obviously cannot have such solutions. Nevertheless, for a global statistical description of the intensity of convective motions Equation (1) may be useful.

Once the function f is determined, Equation (1) can be used to study such things as dependence of convective activity on uncertainty in moisture content. An example of such an application will be given. Also, the effect of random forcing can be studied, which yields another impression on uncertainty in the strength of atmospheric convection.

It is important to note that the convective system that will be modelled by the function f is rather arbitrary, although here it will be based on simulation with a numerical cloud model. Even a two-dimensional cloud model is expensive to run to a state which is statistically steady, and an in-depth investigation of the statistical properties of a moist convective layer is simply impossible. So the strategy will be to gain physical insight from the expensive model and use this to formulate the gradient system. The results obtained in this way should be looked upon as typifying the principal effect of moisture in atmospheric convection, namely, the positive feedback of latent heat release and evaporative cooling, which generate strong motions on a small scale.

2 Calculation of growth rates

In this section we consider some experiments carried out with a numerical cloud model. Although model parameters cannot be varied in a systematic way (this would require too many runs), the experiment is carried out in such a way that the role of the internal forcing can be estimated.

The cloud model to be used is two-dimensional (vertical, horizontal), and simple in the sense that precipitation is not considered explicitly (no formation of ice, but removal of liquid water when the liquid water mixing ratio exceeds a critical value), and that the anelastic Boussineq equation of motion is used (so the only driving force is the buoyancy force). Physics are thus kept to a minimum, which makes it possible to carry out long integrations with reasonable processor times.

The model has been described in VANDELDEN and OERLEMANS (1982) and is in fact rather similar to the one developed by MURRAY (1970). Here only a brief description is given. The dynamics of the model is formulated in terms of a vorticity equation:

$$\frac{\partial \zeta}{\partial t} = -\nabla \cdot \zeta \bar{v} - \frac{\partial B}{\partial x} + K \nabla^2 \zeta; \quad \nabla = \left(\frac{\partial}{\partial x}, \frac{\partial}{\partial y} \right). \tag{2}$$

ζ is the rotation of velocity $\bar{v}$ in the x, z-plane, B is the buoyancy force and K the eddy diffusivity (constant in this study). Conservation of mass is incorporated by introducing a stream function ψ ($u = -\partial\psi/\partial z$, $w = \partial\psi/\partial x$). So the additional equation is

$$\zeta = \nabla^2 \psi. \tag{3}$$

Thermodynamic processes enter Equation (2) through the buoyancy force B, which is calculated from

$$B = g\left[\frac{T_v'}{\overline{T_v}} - r\right]. \tag{4}$$

Here g is the gravitational acceleration, r the liquid water mixing ratio, and T_v the virtual temperature. A bar denotes a value averaged over the x-direction, a prime the deviation from it. Thermodynamics are treat in a Lagrangian way, i. e. the equation

$$c\frac{dT}{dt} = -gw - L\frac{dq_s}{dt} \tag{5}$$

is integrated along air parcel trajectories, which are calculated backwards in time for each grid point. In Equation (5) T is temperature, q_s water vapour mixing ratio at saturation, c specific heat and L heat of condensation.

The numerical scheme further involves the solution of Equation (3) by a relaxation method and time integration of the vorticity equation by means of the Lax-Wendroff method. This combined Eulerian-Langragi method renders the numerical scheme so stable that very long integrations can be carried out without any additional smoothing. In the experiments discussed here a domain size of 4 by 50 km is used, with a 250 m spacing between grid points. The horizontal size of the model domain is rather large, but this was considere necessary to obtain results that estimate the statistical state loosely defined in the Introduction. Mixing is modelled by linear diffusion, with a constant diffusivity for all quantities involved (momentum, water vapour, liquid water, heat), being 25 m^2/s. The time step is 10 s and lateral boundary conditions are cyclic.

In a series of experiments the sensitivity of the growth rate of mean kinetic energy to moisture content of the air was investigated. All integrations were started from an atmosphere at rest, with an initial temperatu profile according to

$$T = 285 - 8.5\ z\ K, \tag{6}$$

where z is the height above the surface in km. The sensible heat flux at the surface was set to 200 W/m^2. To investigate convective activity as a function of moisture content a special arrangement has to be made. The amount of water vapour in the model atmosphere changes as a result of removal of liquid water (precipitation) and of the fact that moisture is not perfectly conserved due to truncation errors. To compensat for this, total moisture content was kept constant by adding after each time step an amount of water vapo equally distributed over all grid points. In general the correction is very small, typically 10^{-4} of the total moisture content per second.

Figure 1a shows results in terms of the mean kinetic energy, for various humidity conditions of the model atmosphere. The labels on the curves give Δ, defines as $T - T_d$, where T_d is the dew point temperature. Varying Δ is of course a rather arbitrary way of changing the amount of moisture, one could also use relative or absolute humidity. However, to find the basic sensitivity of the convection to moisture content variations, this point is not crucial.

Most striking in Figure 1 is the sudden increase in the growth rate of kinetic energy after some time. This increase coincides with the occurrence of the first clouds, and is apparently due to latent heat release. So according to these model results, the transition from the first mode of convection to the second one is quite sharp, even in a model with such a large domain that several clouds may form (a very small random perturbation in temperature is applied at each grid point every time step, so the first clouds form in an independent way). The distribution of cloud water after 45 min real time is shown in Figure 1b for $\Delta = 3$, 4, and 6 K. Apparently the differences are very large. For $\Delta = 3$ K, cloudiness is about 90 %, and practicall all clouds penetrate to the top of the model atmosphere (which is a rigid lid; the difference between a rigid lid and a strong inversion with respect to model behaviour is very small, because gravity waves cannot

• **Bild 1**

(a) Mittlere kinetische Energie als Funktion der Zeit für vier Rechenläufe, die mit einer in Ruhe befindlichen Atmosphäre beginnen. Die Ziffern an den Kurven bezeichnen die einheitlichen Anfangswerte von Δ in K. Der Wärmefluß an der Oberfläche beträgt 200 W m^{-2}.

(b) Wolkenverteilung bei den in (a) gezeigten Modelläufen mit 45 Minuten Simulationszeit.

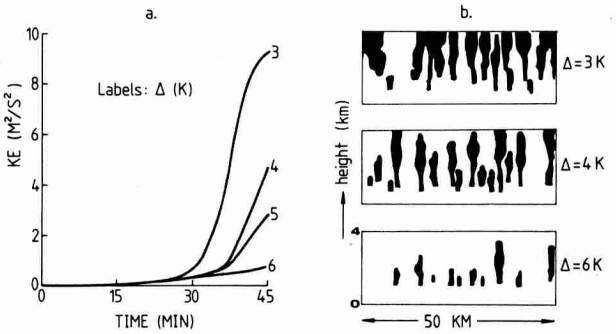

• **Figure 1** (a) Mean kinetic energy as a function of time for four runs starting with an atmosphere at rest. Labels on the curve denote the uniform initial value of Δ(K), and the surface heat flux is 200 W/m^2.

(b) Cloud distribution in the model corresponding to runs shown in (a), after 45 minutes of simulated time.

appear). In contrast, for $\Delta = 6$ K cloud cover is about 20 % and the average cloud depth is much smaller. The runs shown in Figure 1 were continued for 45 min real time only, simply because central processor time is large (1 hr real time simulation requires about 1000 sec on a CDC7600).

3 Formulation of the gradient system

From Figure 1 the growth rate of mean kinetic energy as a function of Δ can be estimated. Attempts to describe the growth rates in terms of surface heat flux and moisture content ultimately led to the following formulation of $\dot{V}$:

$$\begin{aligned} \dot{V} &= cF - \mu V^2 \qquad 0 \leqslant V < V^* \\ \dot{V} &= cF + k(\Delta) - \mu V^2 \qquad V > V^* \end{aligned} \tag{7}$$

Here cF is the growth rate of kinetic energy due to sensible heat input at the surface, a typical value of c is 10^{-6} $m^3/(J\,s)$. The damping is assumed to be quadratic in V. This reflects best the effect of limited depth of the convective layer. Longer runs carried out with a slightly different version of the present numerical model (VAN DELDEN and OERLEMANS, 1982) suggest $\mu = 10^{-3} m^{-1}$. The internal forcing, which comes into operation when V exceeds a critical value V^*, is represented by the function k(Δ). The discontinuous form of $\dot{V}$ is used because it is the best way to represent the very rapid change in growth rates apparent from Figure 1a. As will be illustrated shortly, this introduces bifurcation of the steady state solutions of Equation (7).

It is obvious that the function k(Δ) should be bounded. For $\Delta \to \infty$ the internal forcing should go to zero, and for $\Delta \to 0$ (100 % humidity everywhere) to some finite value. A function fulfilling these requirements and fitting to the growth rates 'observed' from the numerical model is

$$k(\Delta) = a\left[\alpha + \frac{2\alpha}{\pi} \operatorname{arctg}\{\gamma(\delta - \Delta)\}\right], \tag{8}$$

with $a = 10^{-3} m\,s^{-2}$, $\alpha = 4$, $\gamma = 3$ and $\delta = 3.5$ K. So the change of growth rate with Δ is largest around $\Delta = 3.5$ K.

The final refinement to be made is to let V^* increase with Δ, i. e. the critical amount of kinetic energy needed to initiate clouds, and therewith internal forcing, is larger when the atmosphere is dryer. So

$$V^* = \lambda \Delta, \tag{9}$$

where the numerical experiments suggest $\lambda = 0.13\ \mathrm{m\ s^{-1}\ K^{-1}}$. With Equation (8) included, the model now also has the property that for 100 % humidity ($\Delta = 0$) any motion leads to internal forcing.

The gradient system is simple enough to allow the steady states to be determined 'by hand'. First we note that, because V has to non-negative, $V = 0$ while $F < 0$ represents a stable equilibrium by constraint. For $F > 0$ and $V < V^*$, the stable equilibrium state is $V = [c\,F/\mu]^{1/2}$. This stable branche disappears when $[c\,F/\mu]^{1/2} = V^*$, i. e. when

$$\Delta = \frac{1}{\lambda}\left(\frac{c}{\mu}\right)^{1/2} F^{1/2} \tag{10}$$

If V exceeds V^*, the equilibrium state becomes $V = [(cF + k)/\mu]^{1/2}$, which is stable. Inserting Equation (9) we find that this stable branche disappears when

$$\Delta = \frac{1}{\lambda}\,[(cF + k)/\mu]^{1/2}. \tag{11}$$

The last equation is difficult to solve explicitly for Δ, because Δ occurs in the function k in a nonlinear way. However, it can be seen that for F, $\Delta \to \infty$ the curves given by Equations (10) and (11) in the F, Δ control plane approach each other. These curves form the bifurcation set, and for a part of the control plane they are drawn in Figure 2 (upper part). According to the considerations given above, in the shaded

Bild 2

Gleichgewichtszustände des Gradientsystems zur Beschreibung der mittleren konvektiven Aktivität (unten). Die Steuerparameter sind der Feuchtegehalt Δ und der Wärmefluß F an der Oberfläche. Die Lösung besteht aus 3 Flächen: (I) der unteren (dazu gehört auch der Teil, der bei $F = 0$ aufwärts gebogen ist und dann nach rechts weist), diese repräsentiert die trockene Konvektion; (II) der oberen, diese repräsentiert stabile Konvektion mit Wolken; (III) einer Zwischenfläche, diese trennt die stabilen Zustände voneinander (sie kann von der Definition her – hier ist $\dot{V} = 0$ – als ein instabiles Gleichgewicht betrachtet werden). Die dick ausgezogenen Kurven im oberen Bild zeigen die Bifurkation; in dem schraffierten Gebiet zwischen ihnen gibt es zwei stabile Zustände.

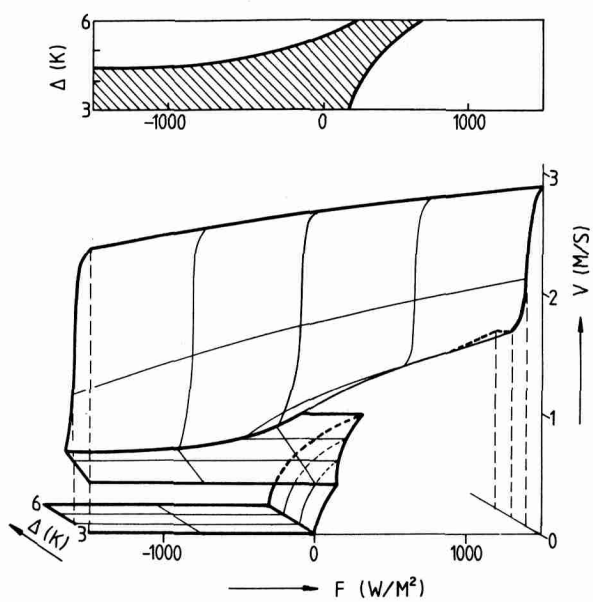

Figure 2 Equilibria of the gradient system describing mean convective activity (lower part). The control parameters are moisture content (Δ), and surface heat flux (F). The solution is made up of three sheets: (I) the lower one (including the part bending upward to the right at $F = 0$) representing dry convection, (II) the upper one representing stable convection with clouds, and (III) an intermediate plane separating the attractor basins of the stable states (it can be considered as an unstable equilibrium by definition, because here $\dot{V} = 0$). Solid lines in the upper panel give the bifurcation set. In the shaded region two stable states occur.

region two stable equilibria exist for any combination of Δ and F. Since in this region $V > 0$ when $V = V^* + \epsilon$ and $\dot{V} < 0$ when $V = V^* - \epsilon$ (ϵ small and positive), it is natural to make $V = V^*$ an unstable equilibrium state *by definition* (this makes sense because, in spite of the fact that $\dot{V}$ is discontinuous at $V = V^*$, the potential of the gradient system can be continuous).

Figure 2 summarizes the analysis. The lower part shows the equilibria of V as a function of the control parameters F and Δ. The upper surface represents the equilibria with internal forcing (i. e. with clouds). The small surface bending upwards to the right from F = 0 represents the dry convection case. The unstable equilibria form a flat surface inclined by an amount λ in the Δ-direction.

So on the basis of growth rates of kinetic energy, calculated with the numerical cloud model, we arrive at a simple gradient system that predicts the existence of multiple statistically steady states for a range of values of moisture content and surface heat flux. Since this result is the essential point of this paper, a further check against the numerical model of moist convection is desirable. To demonstrate the occurrence of two statistically steady states, a number of 3 hr real time simulations were carried out with the surface heat flux F set to zero. In the initial state an upward velocity perturbation of 1 m/s in the middle of the model domain was introduced (otherwise kinetic energy is not generated, in accordance with the simple model). As shown in the right-hand side of Figure 3, three initial moisture profiles were used.

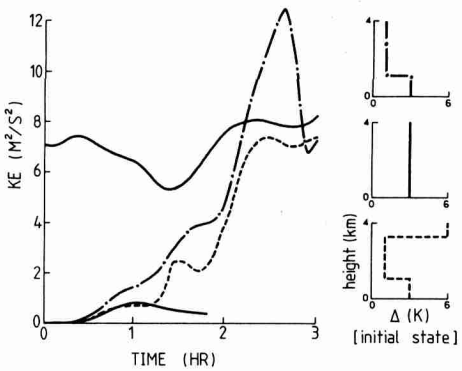

- **Figure 3**
  Runs with zero heat flux at the surface, but with an initial velocity perturbation in the middle of the model domain. The initial humidity profiles are shown at the right.

- **Bild 3**
  Rechenläufe mit F = 0 an der Oberfläche aber mit einer anfänglichen Geschwindigkeits-Störung in der Mitte des Modellgebietes. Rechts werden die anfänglichen Feuchteprofile gezeigt.

Results of these experiments are shown in Figures 3 and 4. In the first run (dot-dashed line in Figure 3) very strong convection developed as a consequence of the large water vapour content. After 160 minutes the mean kinetic energy reached a maximum value of 12 $(m/s)^2$, and slows down somewhat afterwards. The corresponding cloud patterns are displayed in Figure 4, which shows a series with pictures of cloud water mixing ratio. The time interval between the pictures is 15 minutes.

In the next run (dashed line) the upper layer was made much drier. This led to a reduction of the level of kinetic energy, but still large cumulus clouds developed without external forcing. In the third run (lower solid line) the initial velocity perturbation generated a small cloud only, which was not able to initiate the formation of other clouds. However, if the moisture profile of this run (Δ = 3 k everywhere) is again used for an integration with a large amount of *initial* kinetic energy, strong convection is maintained. This is shown by the upper solid line in Figure 3, which refers to a run with the *velocity field* of the dashed run at t = 3 hr as initial condition.

From these experiments it is evident that bifurcation of the statistically steady states as occurring in the simple gradient system is supported by the numerical model. Even when the surface heat flux is zero, the internal forcing easily keeps the convection going when humidity is large enough. Although it is impossible to verify the correctness of the bifurcation set show in Figure 2, the statistical structure of the model atmosphere appears to be formulated well by the simple model discussed in this section.

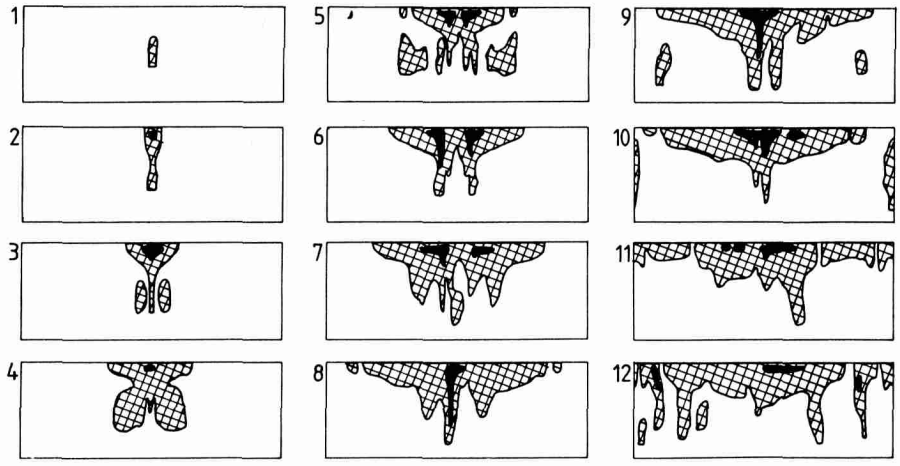

- **Figure 4** Cloud distribution for the .–. run in Figure 3, at 15-minute intervals (the first picture is at t = 15 minutes). In black regions the critical liquid-water content is reached and precipitation occurs.

- **Bild 4** Wolkenverteilung für den –.–-Rechenlauf in Bild 3 nach jeweils 15 min Intervallen (das erste Bild ist für t = 15 r Modellzeit). In den schwarzen Gebieten ist der kritische Flüssigwassergehalt erreicht, und es gibt Niederschlag.

4 Predictability of convection studied with the gradient system

In many situations, a short-range weather forecast depends critically on how well convective ac ity can be predicted. For very dry or very moist conditions predictability is large, of course. In most case however the surface heat flux and moisture content vary in such a way that in the control parameter pla shown in Figure 2 the bifurcation set is frequently crossed. This means that a small perturbation in Δ, sa may lead to a large change in V (and thus in cloud cover). With the simple model derived in the precedin section, this can be investigated further.

In the following the terms convective activity and cloud cover are both used. As will be clear from the experiments with the numerical cloud model, V and cloud cover are related. Whenever V exceeds V^* cl are present and cloud cover will depend on the moisture content and the mean kinetic energy. Figure 5 shows a tentative sketch of how cloud cover depends on Δ and V. This picture fits the behaviour of the atmosphere, as 'observed' from the numerical model, reasonably well (other runs with this model, not discussed here, have helped to construct Figure 5). For the following discussion the point of how the oc rence of clouds is related to V is not crucial, because all results will be given in terms of V. It may help t interpret the results, however.

Suppose that predictions of Δ are normally distributed around the observed values with some standard deviation σ_Δ. The question than is to find out how this uncertainty in Δ affects the prediction of V. Th point was studied with the Monte Carlo technique. For a given surface heat flux and with initial conditio V = 0 a series of 200 integration was carried out in which the value of Δ was drawn from a normal distribu tion with $\sigma_\Delta = 0.5$ K. So this procedure yielded 200 functions $V_i(t)$, and the interest concerns the varia tions between the V_i. To display the results in an orderly fashion, histograms were computed for every 15 minutes. Placing these histograms behind each other then gives an impression of how the probability distribution of V (which is just a spike at t = 0) evolves in time. The V-axis is split up in intervals of 0.1 m/s width. This yields the pictures shown in Figure 6. Results are given for mean values of Δ of 3 an 4 K, and for various values of the surface heat flux.

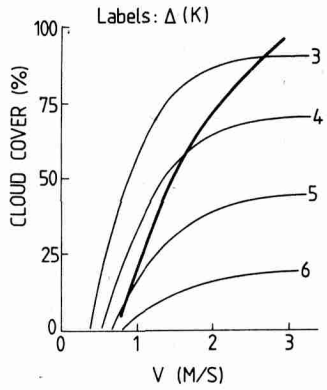

- **Figure 5**
  Tentative relation between cloud cover and rms velocity V, for various moisture conditions. A typical corresponding surface heat flux is 100–150 W/m^2. The equilibrium states lie on the solid line.

- **Bild 5**
  Versuchsweise aufgestellte Beziehung zwischen Bedeckungsgrad und Standard-Abweichung der Geschwindigkeit für verschiedene Feuchtebedingungen. Ein typischer entsprechender Wärmefluß an der Oberfläche ist 100–150 W m^{-2}. Die Gleichgewichtszustände liegen auf der dick ausgezogenen Linie.

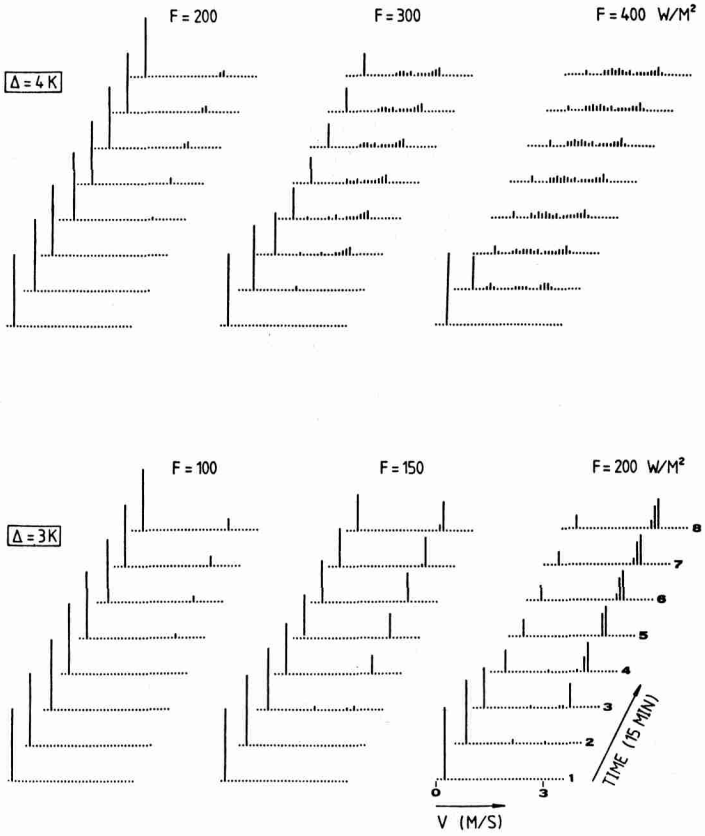

- **Figure 6**
  Probability distributions of V (interval 0.1 m/s) as a function of time. The initial state is a spike at V = 0.

- **Bild 6**
  Wahrscheinlichkeits-Verteilungen von V (Intervall 0.1 m s^{-1}) als Funktion der Zeit. Der Anfangszustand ist eine Spitze bei V = 0.

In the pictures the tendency towards a bimodal distribution is clearly seen, in particular for moist conditions ($\Delta = 3$ K). For $\Delta = 3$ K and F = 150 W/m^2, the probability of an almost clear sky is about just as large of that of an almost completely cloud-covered atmosphere with shower activity. For somewhat drier conditions ($\Delta = 4$ K), the distribution of V becomes rather flat when the surface heat flux is large. Note that for F = 400 W/m^2 a dip occurs in the middle of the range that represents convection with clouds. This dip corresponds to the steepest part of the upper sheet in Figure 2.

Analogous experiments concerning uncertainty in the surface heat flux and initial state can easily be carri out, and give in fact similar results: in 'extreme cases' predictability is large, and for intermediate conditions (typical for the midlatitude atmosphere) it is low (that is, if a bimodal distribution is considered to reduce the practical predictability for a meteorologist; she/he cannot state that tomorrow the weather wil be either either very sunny or rainy, but will use a formulation like 'sunny weather with a small risk of a shower'). In this sense bifurcation in a system reduces the predictability (in fact because an unstable stead state is introduced).

A further example is shown in Figure 7. In this case the surface heat flux varies sinusoidally with a period of 24 hr and has an amplitude of 200 W/m^2. Again the initial (t = 0) probability distribution of V is a spike at V = 0. The standard deviation of V, which can be considered as some measure of predictability, is also shown. In the case shown, predictability decreases rapidly when the surface heat flux increases, and after a few hours settles at a rather constant level.

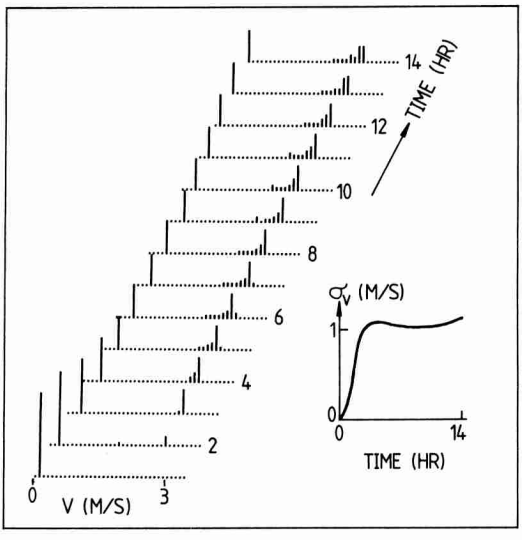

- **Figure 7**
  Evolution of the probability distribution for a typical day with strong heat flux and substantial moisture content (Δ = 3.5 K). The standard deviation of V as a function of time is also shown.

- **Bild 7**
  Entwicklung der Häufigkeitsverteilung für einen typischen Tag mit großem Wärmefluß und Feuchtegehalt (Δ = 3.5 K). Die Standard-Abweichung von V als Funktion der Zeit ist rechts unten dargestellt.

5 Random forcing

Many other experiments can be done with the simple model. For instance, a stochastic forcing $\epsilon(t)$ can be added to represent the action of processes that are not explicitly taken into account. Such processes could be forcing of vertical motions by orography, changing in the nature of the underlying surface, etc. Equation (7) then becomes

$$\dot{V} = cF + k - \mu V^2 + \epsilon(t) \qquad (12)$$

Since the structure of the model is rather simple, some inferences can be made on the basis of experiments carried out with stochastically forced simple deterministic systems in climate dynamics (FRAEDRICH, 197 NICOLIS and NICOLIS, 1979; BENZI et al., 1981; among others).

When the strength of the random forcing is very large (relative to the potential barrier between the stable equilibria) the probability distribution of V will be unimodal, and the fact that for some values of the surface heat flux and moisture content multiple equilibria exist is unimportant. Such a situation may for exa ple arise when an air stream is hitting the complex mountain and valley systems of the Alps.

For weaker forcing, i. e. a forcing that is such that the probability of crossing the potential barrier between the stable states is substantially reduced, the probability distribution of V can be either unimodal or bimodal, depending on the heat flux and moisture content.

In the latter case the system switches every now and then from the environment of one stable equilibrium to that of the other stable equilibrium, and trajectories in phase space look like trajectories of a Lorenz attractor.

In an attempt to generalize a typical midlatitude situation, we consider an experiment in which moisture content varies according to red noise and the daily cycle is included in the upward heat flux F. Moisture content is calculated from

$$\dot{\Delta} = \frac{\Delta_m - \Delta}{T} + \delta(t) \tag{13}$$

The relaxation time T is set to 10^5 sec (= 1.16 day), and Δ_m to 5 K. The strength of the white-noise proces $\delta(t)$ is chosen in such a way that σ_δ = 1.5 K. The daily cycle in the surface heat flux is represented by mean of a sinus function with an amplitude of 300 W/m^2, and the strength of $\epsilon(t)$ in (12) is σ_ϵ = 0.2 m/s.

Equations (12)–(13) can be thought of as describing in a very schematic way the history of an air mass travelling around in summer, pickung up or loosing moisture, and subject to forcing by a periodic heat flux and a (small) random upward momentum flux.

Integrating this system leads to the pictures shown in Figure 8. V is plotted as a function of time of the day; every 12 minutes a spot is plotted. The upper left panel shows the evolution of V for just one arbitrary day. The other panels give results for 20 days of simulated time, they differ with respect to the random number set that was used. In the lower right panel only situations with clouds (i. e. internal forcing not zero) are plotted.

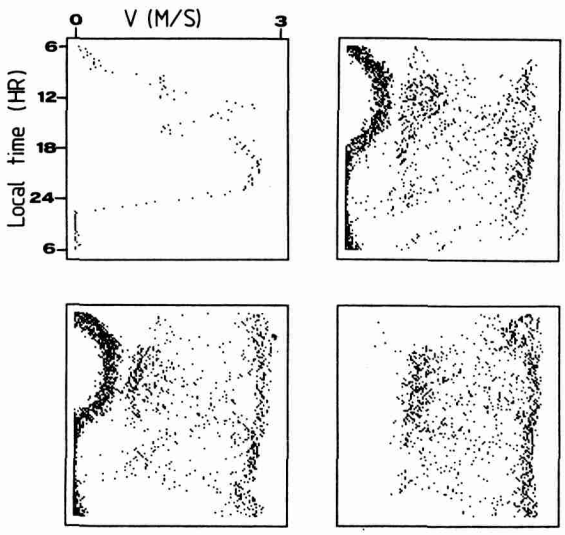

Bild 8

V als Funktion der Zeit. Das Gradientsystem wird angetrieben von einem periodischen Oberflächen-Wärmefluß und Schwankungen (rotes Rauschen) im Feuchtegehalt. Ein Tagesgang für einen Tag ist oben links zu sehen. Die anderen Bilder zeigen Ergebnisse von Integrationen über 20 Tage; sie unterscheiden sich nur in dem Satz der Zufallszahlen, der zur Erzeugung des roten Rauschens benutzt wurde. In allen Bildern wurde alle 12 min ein Punkt gezeichnet. Im unteren rechten Bild wurden nur dann Punkte eingezeichnet, wenn Wolken vorhanden waren.

Figure 8 Plots of V as a function of local time. The gradient system is forced by a periodic surface heat flux and red-noise fluctuations in moisture content. A one-day history is shown in the upper left. The other panels give results for 20-day integrations; they only differ with respect to the random-number set used in the generation of the red noise. In all pictures a spot was plotted every 12 minutes. In the lower right panel spots were only plotted when clouds were present.

The band with a high density of spots reflects the direct response to the surface heat flux. Apart from this, clustering occurs for $2.5 < V < 3$ m/s, corresponding to high cloudiness conditions and strong internal forcing. There the daily cycle in F apparently plays a minor role: once the convective activity has reached a certain level, it can survive during the night in many cases.

Another cluster occurs for $V \simeq 1$ m/s, centered around noon or a little bit later. Here we find the 'fair weather cumulus' regime, appearing for moderately dry conditions. In most cases, the level of convective activity goes down later in the day and internal forcing then ceases.

6 Summary

That internal forcing of convection by latent heat release is important has already been known for a long time. In this paper an attempt has been made to quantify this forcing in some kind of statistical way. To find a simple gradient system, a number of runs with a dynamical cumulus cloud model have been analyzed. A cloud model is expensive in use, certainly if a large domain is chosen, and the number of experiments that can be carried out is thus limited. For that reason the 'convective system' studied in this paper is rather arbitrary.

In spite of this, the results obtained probably characterize the nature of a moist convective atmosphere quite well. Proper scaling may yield a wider applicability, for instance Δ could be replaced by total moisture content in a column to introduce the effect of the depth of the convective layer.

An important result is that a probability distribution of convective activity shows a tendency towards a bimodal shape. This bimodal shape is likely to be one of the reasons that skill-scores for forecasts of precipitation and cloudiness are much lower than for temperature and wind. Of course the picture is considerably obscured by the fact that stratiform clouds play an important role too. Still the present paper illustrates that in many situations 'internal forcing' due to latent heat release reduces in a substantial way the possibility of making a short-range weather forecast.

Acknowledgements

I thank Cor SCHUURMANS, Erland KÄLLEN, Aarnout VAN DELDEN and the referees for useful comments on earlier versions of this article.

References

ARAKAWA, A. and W. H. SCHUBERT, 1974: Interaction of cumulus cloud ensemble with the large-scale environment. J. Atmos. Sci. 31, 1232–1240.

BENZI, R., G. PARISI, A. SUTERA and A. VULPIANI, 1982: Stochastic resonance in climatic change. Tellus 34, 10–16

BROWNING, K. A. and F. H. LUDLAM, 1962: Airflow in convective storms. Quart. J. Roy. Met. Soc. 88, 117–135.

DRIEDONKS, A. G. M., 1981: Dynamics of the well-mixed atmospheric boundary layer. Royal Netherlands Meteorological Institute, Scientific Rep. 81–82.

FRAEDRICH, K., 1978: Structural and stochastic analysis of a zero-dimensional climate model. Quart. J. Roy. Met. Soc. 104, 461–474.

GATES, W. L., 1981: The climate system and its portrayal by climate models. In: Climatic Variations and Variability: Facts and Theories (Ed.: A. BERGER), Reidel, 3–20.

GILMORE, R., 1981: Catastrophe theory for scientists and engineers. John Wiley, New York.

KITCHEN, M. and S. J. CAUGHEY, 1981: Tethered balloon observations of the structure of small cumulus clouds. Quart J. Roy. Met. Soc. 107, 853–874.

KUO, H. L., 1974: Further studies of the parameterization of the influence of cumulus convection on large-scale flow. J. Atmos. Sci. **31**, 1232–1240.

MILLER, M. J., 1978: The Hampstead storm: a numerical simulation of a quasi-stationary cumulonimbus system. Quart. J. Roy. Met. Soc. **104**, 413–427.

MONCRIEFF, M. W., 1978: The dynamical structure of two-dimensional steady convection in constant vertical shear. Quart. J. Roy. Met. Soc. **104**, 543–567.

MONCRIEFF, M. W., 1981: A theory of organized steady convection and its transport properties. Quart. J. Roy. Met. Soc. **107**, 29–50.

MURRAY, F. W., 1970: Numerical models of a tropical cumulus cloud with bilateral and axial symmetry. Mon. Weather. Rev. **98**, 14–28.

NICOLIS, C. and G. NICOLIS, 1981: Stochastic aspects of climatic transitions – additive fluctuations. Tellus **33**, 225–234.

TELFORD, J. W. and J. WARNER, 1962: On the measurement from an aircraft of bouancy and vertical air velocity. J. Atmos. Sci. **19**, 415–423.

VAN DELDEN, A. and J. OERLEMANS, 1982: Grouping of clouds in a numerical cumulus convection model. Beitr. Phys. Atmosph. **55**, 239–252.